Toxicology in Vitro 96 (2024) 105772

Contents lists available at ScienceDirect

Toxicology in Vitro

journal homepage: www.elsevier.com/locate/toxinvit

Particulate iron oxide food colorants (E 172) during artificial digestion and their uptake and impact on intestinal cells

Holger Sieg [a,*], Caroline Schaar [a], Nicole Fouquet [a], Linda Böhmert [a], Andreas F. Thünemann [b], Albert Braeuning [a]

[a] German Federal Institute for Risk Assessment, Department of Food Safety, Max-Dohrn-Straße 8-10, 10589 Berlin, Germany
[b] German Federal Institute for Materials Research and Testing (BAM), Unter den Eichen 87, 12205 Berlin, Germany

ARTICLE INFO

Editor: Dr I Maschmeyer

Keywords:
Iron oxide nanoparticles
Food colorant
E 172
Cellular effects
Artificial digestion

ABSTRACT

Iron oxide of various structures is frequently used as food colorant (E 172). The spectrum of colors ranges from yellow over orange, red, and brown to black, depending on the chemical structure of the material. E 172 is mostly sold as solid powder. Recent studies have demonstrated the presence of nanoscaled particles in E 172 samples, often to a very high extent. This makes it necessary to investigate the fate of these particles after oral uptake. In this study, 7 differently structured commercially available E 172 food colorants (2 x Yellow FeO(OH), 2 x Red Fe_2O_3, 1 x Orange Fe_2O_3 + FeO(OH) and 2 x Black Fe_3O_4) were investigated for particle dissolution, ion release, cellular uptake, crossing of the intestinal barrier and toxicological impact on intestinal cells. Dissolution was analyzed in water, cell culture medium and artificial digestion fluids. Small-angle X-ray scattering (SAXS) was employed for determination of the specific surface area of the colorants in the digestion fluids. Cellular uptake, transport and toxicological effects were studied using human differentiated Caco-2 cells as an *in vitro* model of the intestinal barrier. For all materials, a strong interaction with the intestinal cells was observed, albeit there was only a limited dissolution, and no toxic *in vitro* effects on human cells were recorded.

1. Introduction

Iron is a highly abundant trace element in human nutrition, necessary for many essential and vital functions (Erdman et al., 2012). One important form is contained in the heme molecule, which is part of a number of vital proteins and structures like hemoglobin, myoglobin, and cytochrome. Moreover, there are numerous enzymes associated with iron, for example cytochrome P450, cytochrome *c* reductase, catalases, peroxidases and glucose-6-phosphate dehydrogenase. The total iron content in the body is about 3 to 5 g with most of it in the blood, liver, bone marrow, and muscles. The Population Reference Intake (PRI) for iron is 11 mg/day for adult men ≥18 years and postmenopausal women, and 16 mg/day for premenopausal women, including pregnant and lactating women (EFSA Scientific Committee, 2015a). EFSA considered the then available data inadequate for derivation of a Tolerable Upper Intake Level (UL); however, based on adverse gastrointestinal effects, the former US-Institute of Medicine (IOM) set a UL for males and females ≥14 of 45 mg/day (IOM, 2001). The homeostasis of iron maintains the iron levels in serum within physiological range only by upregulation or downregulation of absorption mechanisms of iron. This means that it maintains homeostasis by regulating only the absorption of iron, but not the excretion, as there are no active pathways to excrete iron (Bhattacharya et al., 2016). For food supplements, the German Federal Institute for Risk Assessment (BfR) names a recommended maximum level of 6 mg iron per day (BfR, 2021).

Chronic iron overload may, however, occur as a result of specific clinical conditions and genetic mutations (EFSA Scientific Committee, 2015a), but also long-term excessive supplement intake (Lands and Isang, 2017; McDowell et al., 2018). In addition to the natural iron intake from food ingredients, iron oxide is authorized as food additive E 172 in the European Union and used as food colorant for example in sweets, olives and cheese rind (European Commission, 2008; EFSA Scientific Committee, 2015b). Depending on the chemical structure, material properties can change and especially the color can range from yellow (FeO(OH)), orange (FeO(OH) + Fe_2O_3), red (Fe_2O_3) to black (Fe_3O_4) (Cornell and Schwertmann, 2003), which are all classified as E

* Corresponding author.
E-mail addresses: holger.sieg@bfr.bund.de (H. Sieg), linda.boehmert@bfr.bund.de (L. Böhmert), andreas.thuenemann@bam.de (A.F. Thünemann), albert.braeuning@bfr.bund.de (A. Braeuning).

https://doi.org/10.1016/j.tiv.2024.105772
Received 19 September 2023; Received in revised form 22 November 2023; Accepted 5 January 2024
Available online 8 January 2024

172 regardless to their color and chemical structure. These materials are commercially available for industrial and private purposes and are often sold as solid powders. Recently, it was discovered that these materials can contain a significant fraction of particles in the nanometer range (1 to 100 nm) (Voss et al., 2020a). Due to European authorities, intentionally produced nanomaterials and the application of nanotechnologies is subjected to a specific regulation (EFSA Scientific Committee, 2021a). Furthermore, conventional materials which contain a nano-scaled fraction underlie a guidance on technical requirements for regulated food and feed products (EFSA Scientific Committee, 2021a). Because of their size and the thereof resulting nano-specific properties, physico-chemical as well as toxicological effects of nanoparticles can differ strongly from conventional materials (Oberdorster et al., 2007; Ray et al., 2009). Their cellular uptake and bioavailability can vary due to nano-specific mechanisms to overcome biological barriers in the body (Yameen et al., 2014). This gives nanocompounds a potential in supplementing nutrition, but likewise this leads to the concern, whether iron oxide nanoparticles on top on the daily ionic iron amount can cause toxic effects after oral uptake (Zimmermann and Hilty, 2011; Garcia-Fernandez et al., 2020). This makes a detailed investigation on both, cellular uptake and effects of nanoparticle-containing materials necessary. Moreover, most *in vitro* studies on nanoparticles are a first good step to replace animal studies, but they lack the influence of the fluids present in the upper intestinal tract, namely saliva, gastric juice and intestinal juice. This is highly relevant, because an important material characteristic is the dissolution behavior in biological fluids (EFSA Scientific Committee, 2021b). Nanoforms of various materials showed strong differences in solubility in artificial digestion experiments, underlining the importance of these investigations (Voss et al., 2019; Sieg et al., 2017; Bohmert et al., 2014; Sohal et al., 2018a). Even though iron is considered to pose overall a low risk to human health (JECFA, 1980), the fate and behavior of iron-containing nanoparticles in the human body is still unclear and needs further investigation (Zimmermann and Hilty, 2011; Sohal et al., 2018b).

In this study, it was our aim to obtain information on following questions by using commercially available E 172 food colorant samples. This included the behavior of food colorants in the intestinal fluids during digestion, their cellular interactions with epithelial cells, their crossing over the intestinal epithelial barrier, and their toxicological effects intestinal epithelial cells. Therefore, seven different E 172 iron oxide containing food colorants (two yellow, two red, one orange and two black food dyes), in which nanoscaled fractions of particles are present, have been chosen and investigated extensively with regard to their material characteristics (Voss et al., 2020a). All materials are commercially available on the market and are used for food coloring applications. First of all, their ion release in water, cell culture medium and artificial digestion fluids was measured. A well-established artificial digestion system was used to simulate the conditions of saliva, stomach fluid and intestinal fluid (Versantvoort et al., 2005; Sieg et al., 2017; Voss et al., 2021). Furthermore, lecithin, as the commonly used food emulsifier E322 was used to investigate the influence on agglomeration behavior during digestion (European Commission, 2008). Small Angel X-ray Scattering (SAXS) as a standardized method for *in situ* particle size analyses (ISO 17867, 2020), determination of particle number concentration (ISO/FDIS 23484, 2022) and specific surface areas (ISO 20804, 2022) was used for characterization. Secondly, a Caco-2 based *in vitro* model was applied to simulate the human intestinal barrier in a Transwell® system (Fogh et al., 1977; Buhrke et al., 2011; Hidalgo et al., 1989). This makes it possible to quantify cellular uptake and barrier crossing of test substances. Thirdly, the toxicological tests were applied on this intestinal cell model.

2. Materials and methods

2.1. Chemicals and test substances

Standard chemicals were purchased from Sigma-Aldrich (Taufkirchen, Germany), Merck (Darmstadt, Germany), or Carl Roth (Karlsruhe, Germany) in the highest available purity. ZnO nanoparticles were supplied by IoLiTec (Heilbronn, Germany). E 172 food colorants were obtained by different commercial suppliers and are used for industrial and private food coloring processes. The brands are known by the authors and are available upon request. E 172 food colorants and ZnO nanoparticles were freshly dispersed prior to use according to the modified NanoGenoTOX protocol (dispersion in 0.05% bovine serum albumin (BSA)/water by ultrasonication with KE76 tip for 5′09″ with ~20% energy) (NanoGenoTOX, 2011). BSA was supplied by Carl Roth (Albumin Fraction V, ≥98%). The respective iron content of each food colorant stock dispersion is presented in Table S 1. For food colorant Red 2, due to its low initial iron content, a three-fold amount of powder was used for dispersion. The physico-chemical characteristics and applied concentrations of the food colorants can be found in Table S 1 and in (Voss et al., 2020a).

2.2. Element analysis

The amount of free Fe ions was determined by atomic absorption spectroscopy (AAS). Stock dispersions were diluted into water or cell culture medium and immediately used or incubated for 24 h at 37 °C / 5% CO_2. The ionic amount of Fe in stock solutions, cell culture media or artificial digestion fluids was determined by ultracentrifugation (100,000 x*g* for 1 h at 4 °C) followed by acidic hydrolysis of the supernatant (69% HNO_3, 180 °C for 20 min in an MLS-ETHOS Microwave system, MLS Leutkirch, Germany) and element analysis by AAS (Perkin Elmer PinAAcle 900, Perkin Elmer, Waltham USA). The methods were previously published (Sieg et al., 2018; Voss et al., 2021). Results are given as percentile of the initially applied amount of Fe. Fe background was determined in water and cell culture medium using samples without additional Fe. Total iron recovery experiments are shown in Fig. S 1.

2.3. Artificial digestion

The artificial digestion was performed according to previously optimized protocols which contain fluids simulating the physical and chemical conditions of saliva, stomach fluid and intestinal fluid including their buffer conditions, pH values, enzyme compositions and duration times (Sieg et al., 2017; Voss et al., 2021). Experimental volumes and buffer compositions are depicted in Fig. 1. In this study, for artificial digestion one E 172 food colorant of each color (Yellow 2, Red 1, Orange, and Black 2) was chosen. Each food colorant was digested with an initial concentration of 0.33 mg Fe/mL in artificial saliva and 0.05% BSA added as a stabilizer. As a further supplement, the food colorants were digested with and without lecithin, a natural emulsifier. Lecithin, as a commonly used emulsifier, was chosen to investigate, whether its presence can have an influence on particle agglomeration and dispersion stability. Furthermore, a digestion control without additional iron was used with and without lecithin. The artificial digestion of the pigment Yellow 1 was already performed and published in a previous study (Voss et al., 2021). Enzyme activity was tested after each digestion step to ensure the functionality of the digestion enzymes (not shown).

2.4. Small-angle X-ray scattering (SAXS)

SAXS measurements were conducted in a flow-through capillary with a Kratky-type instrument (SAXSess from Anton Paar AG, Graz, Austria) at a temperature of 21 ± 1 °C. The SAXSess has a low sample-detector-distance of 0.309 m which is appropriate for the investigation

Composition of digestion fluids [mg/mL]		
Saliva pH 6.4	Gastric Juice pH 2.0	Intestinal Juice pH 7.5
1.667 NaCl	4.143 NaCl	0.3 NaCl
0.5 NaSCN	1.0 KCl	0.5 NaSCN
1.833 Na_2SO_4	0.386 KH_2PO_4	0.5 $NaHCO_3$
0.5 $NaHCO_3$	4.286 Mucin	0.3 Trypsin
1.5 KCl	1.429 Pepsin	0.3 Ureate
2.0 KH_2PO_4	HCl for titration	0.5 $CaCl_2 \cdot H_2O$
0.5 $CaCl_2 \cdot H_2O$		0.2 $MgCl_2 \cdot 6\ H_2O$
0.33 Ureate		9.0 Pancreatin
0.033 Urea		9.0 Bile extract
0.833 α-Amylase		$NaHCO_3$ (s)
2.5 Mucin		for titration

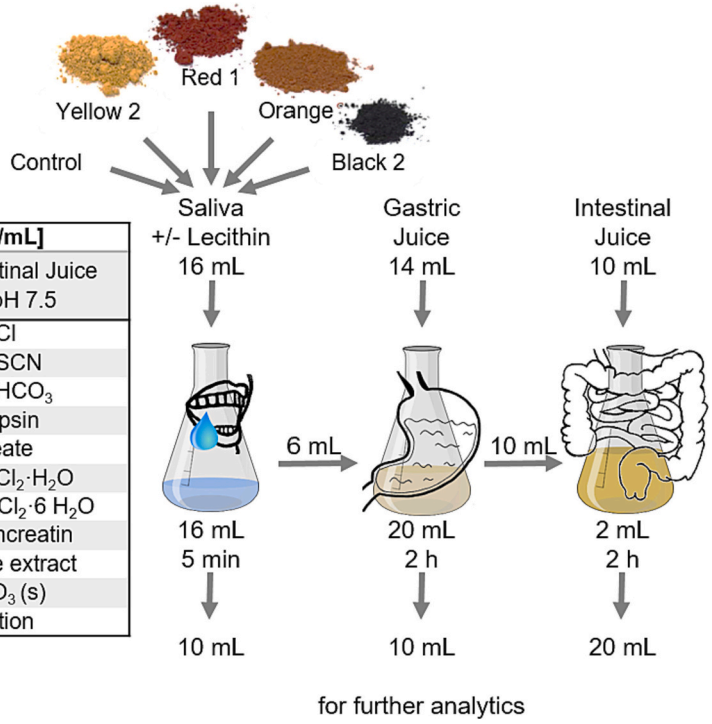

Fig. 1. Scheme of the artificial digestion procedure (left) and buffer compositions of each digestion step (right). The artificial digestion fluids were constantly stirred at 37 °C. The depicted volumes were successively added and removed for further analysis.

of dispersions with low scattering intensities. The artificially digested samples were measured without any further sample treatment as they were taken from the digestion vessels. Samples in cell culture medium were diluted into DMEM (High Glucose, 10% FBS, 1% Pen/Strep.) to a concentration of 50 µg Fe/mL and incubated for 24 h at 37 °C and 5% CO_2 prior to measurement. The experiments were performed with 120 measurement cycles (each averaged over 10 s). The measurements were background-corrected with the respective digestion fluid. Deconvolution (slit length desmearing) of the SAXS data was performed with the SAXS-Quant software (Anton Paar AG). Analysis of the SAXS data and calculation of the scattering contrasts were performed with the software SASfit as described before (Bressler et al., 2015). Calibration of the intensity to absolute scale was performed using water as secondary standard (Orthaber et al., 2000).

2.5. Cell cultivation

Caco-2 cells were cultivated in DMEM High Glucose with 10% fetal calf serum (FCS) and 1% penicillin/streptomycin (P/S) (GE Healthcare, Solingen, Germany, passages 20+, maximum 9 passages after thawing). 5000 Caco-2 cells were seeded into each cavity of 96-well plates and xCELLigence® *E*-plates, and 50.000 cells on Transwell® membranes in 12-well format, respectively. Proliferating (prol.) Caco-2 cells were used for experiments 24 h after seeding. For differentiation, in every format, medium was changed every 2–3 days for a differentiation time of 21 days. As incubation volumes, 100 µL (96-well and E-plate, prol. Caco-2), 200 µL (E-plate, diff. Caco-2), 300 L (96-well, diff. Caco-2) and 500 L (Transwell® apical compartment) were used.

2.6. Cellular assays

Cell viability was determined by the MTT assay for proliferating Caco-2 cells in 96-well plates. Cells were incubated with freshly dispersed, undigested test substances, and controls for 24 h prior to measurement. After the incubation time, 10 µL 5 mg/mL 3-(4,5-dimethylthiazol-2-yl)-2,5-diphenyltetrazolium bromide (MTT) in PBS were added for another 1 h. After that, the entire medium was removed and 130 µL pre-warmed desorption agent (0.7% *w/v* SDS in isopropanol) were added. Plates were shaken for 30 min and absorption was measured on a plate reader (570 nm) with subtraction of the background absorption (630 nm). As control for cytotoxicity, 0.01% Triton X-100 was used.

Cellular impedance was determined by an xCELLigence® system (xCELLigence®, Roche, Germany). Caco-2 cells were seeded in special gold-coated 96-well *E*-plates and incubated with the test substances, either with 100 µL starting 24 h after seeding in the case of proliferating Caco-2 cells, or with 200 µL for differentiated Caco-2 cells after 21-day differentiation. Samples were measured over a time period of 72 h. As toxic positive control, ZnO nanoparticles (50 µg Zn/mL) were used. The cell indices were determined in at least 3 replicates for each condition and are depicted as mean values with standard deviation.

2.7. Transport studies

For transport studies, differentiated Caco-2 cells were incubated with E 172 food colorants (50 µg Fe/mL in 500 µL sample volume, applied to the apical compartment for 24 h). After that, membrane integrity was checked by TEER measurements and a FITC-dextran permeability assay as described before (Sieg et al., 2018) (data not shown). The basolateral fractions were harvested to determine Fe transport, while the membranes with cells were washed with PBS and harvested by cutting off with a scalpel. The wash fraction was added to the apical fraction. All fractions (basolateral, apical / wash, membrane) were chemically digested and Fe contents were determined by AAS as described above. Natural background of Fe was determined by measuring medium and cell samples without additional Fe. Uptake and transport of Fe is depicted as percentage of the applied Fe amount. Total iron recovery experiments are shown in the supporting information (Fig. S 2).

2.8. Statistics

For cell viability measurements, results were normalized to medium

controls after subtraction of equally treated cell-free reference wells. Statistics were performed with the results of at least 3 independent experiments by Student's *t*-test compared to medium controls. Statistical significance is indicated by asterisks (* $p < 0.05$; ** $p < 0.01$; *** $p < 0.001$).

3. Results

3.1. Material characteristics during artificial digestion

In contrast to other research on iron oxide nanoparticles, the herein presented work is done on commercially available food colorants, containing a nanoscaled fraction of particles. Seven different E 172 iron oxide containing food colorants (two yellow, two red, one orange and two black food dyes), which are available on the international market, were chosen and characterized extensively as published previously by Voss et al. and summarized in Table S1 in the supporting information (Voss et al., 2020a). These colorant powders were now used in an artificial digestion and *in vitro* cell culture experiments. To evaluate the further fate of these nanoparticle-containing food colorants after oral uptake, it is important to determine their solubility and ion release into different liquid media with increasing complexity, namely water, cell culture media (DMEM High Glucose with 10% FCS and 1% P/S) and the fluids of the upper intestinal tract (saliva, gastric juice and intestinal juice).

Fig. 2 shows the individual dissolution behavior of each food colorant after 24 h in water [A] and cell culture medium [B] by the determination of their fraction of released Fe ions. In water, only an extremely low percentile of below 0.02% of the added Fe was measurable in the ionic fraction, showing no differences among the 7 different investigated E 172 samples. In cell culture medium, the measured ionic Fe content was still very low, but higher than in water, with percentiles between 0.3 and 0.7%. The relatively highest concentrations of free Fe ions in cell culture medium were measured for the black E 172 pigments, but still the margin of error, with regard to the other pigments. In all cases, the measured Fe amount did not notably exceed the previously determined free ionic Fe backgrounds (0.01% / 0.005 µg Fe/mL for water, 0.46% / 0.23 µg Fe/mL for cell culture medium). The correctly applied Fe contents were confirmed by recovery measurements, shown in Fig. S 1.

One E 172 food colorant of each color was chosen for the previously explained artificial digestion simulation (Yellow 2, Red 1, Orange, Black 2). After each digestion step, samples were taken to determine their free ionic Fe content (Fig. 2C). To assess the influence of additional emulsifiers, the same analysis was also performed in presence of lecithin (Fig. 2D). All samples showed a very low dissolution with ionic amounts below 1% of the added Fe, indicating no relevant dissolution with no differences between each E 172 compound, and no substantial effect of lecithin addition. The ionic backgrounds in the control samples were determined as well, shown as gray dashed lines for each digestion step. The free ionic Fe amount did not remarkably exceed the determined background levels of the digestion fluids.

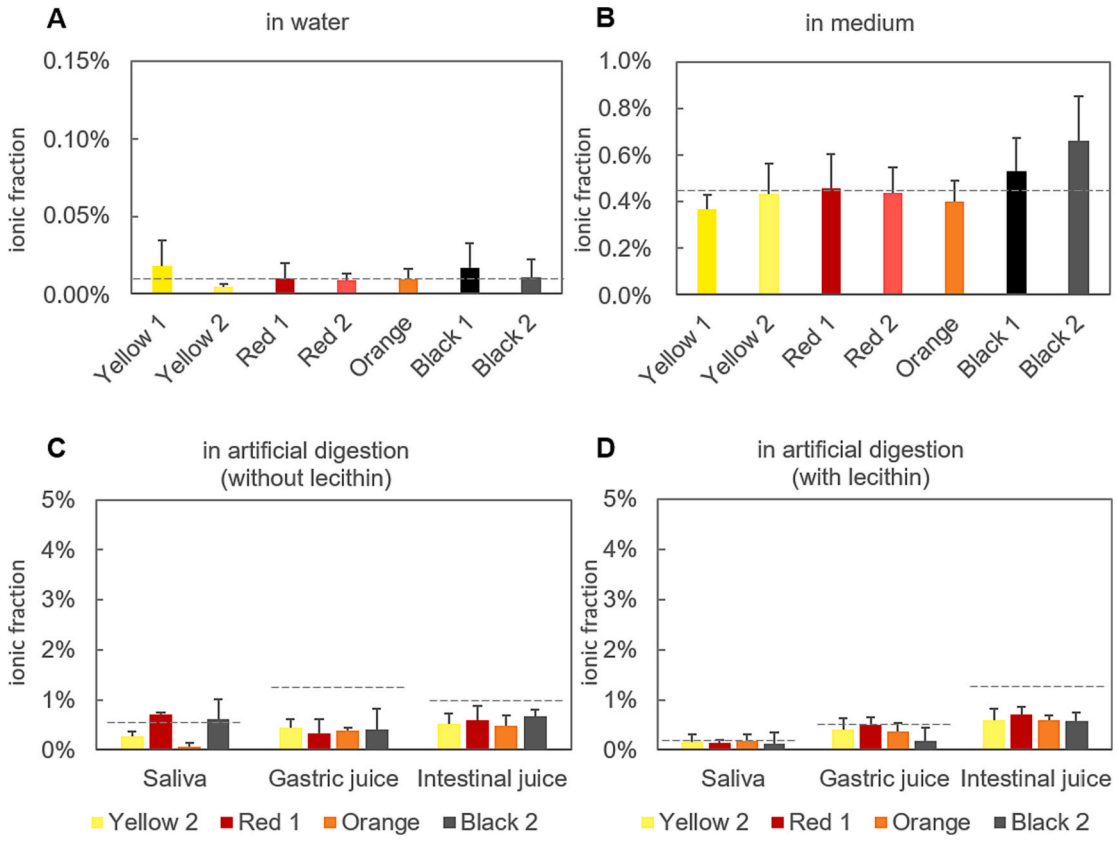

Fig. 2. Ionic iron content in [A] water and [B] cell culture medium after an incubation time of 24 h, after ultracentrifugation and subsequent element analysis by AAS. Results are shown as relative ionic iron content [%] compared to the theoretically applied iron concentration of each E 172 food colorant (50 µg Fe/mL). Iron backgrounds of water and cell culture medium (dashed lines) are also depicted. Results are shown as mean values of at least 6 samples and error bars indicate standard deviation. Total iron recovery is shown in Fig. S 1; Ionic iron content in artificial digestion fluids [C] without lecithin and [D] with lecithin, measured by ultracentrifugation and element analysis by AAS: Results shown as relative ionic iron content [%] compared to the theoretical applied iron content of each E 172 food colorant. Iron backgrounds of each digestion fluid (dashed lines) were determined from digestion control samples without additional iron and are depicted as [%] of the additionally added iron amount. Results shown as mean values of at least 3 replicates and error bars indicating standard deviation.

3.2. SAXS results of the digestion experiments

The SAXS intensities $I(q)$ of all samples decay accordingly to Porod's law (Porod, 1951) asymptotically with the inverse forth power of the scattering vector q as

$$I(q) = A + K\,q^{-4}$$

where A denotes a constant scattering background and the parameter K contains information on the surface of the pigments. With K, the specific surface can be calculated as

$$S_m = \frac{K}{2\,\pi\rho_s\Delta\rho^2}$$

where $\rho_s$is the density of the pigment and $\Delta\rho$ is the scattering contrast between pigment and medium. The SAXS data of Yellow 2 and curve fits are provided as examples in Fig. 3. Higher scattering intensities are visible in the line "saliva", "stomach" and "intestine" for a q-range of 0.068 nm^{-1} to 0.70 nm^{-1} and accordingly, the specific surface increases in the line 8.2 ± 0.4 $m^2\,g^{-1}$, 16.8 ± 0.9 $m^2\,g^{-1}$, 38.2 ± 2.0 $m^2\,g^{-1}$. An overview on all specific surface areas is given in Fig. 4. The overall trend is that the specific surface area of the pigments is greatest in the intestinal compartment. For comparison, we investigated the pigments after incubation in cell culture medium for 24 h. The curve fits, shown in Fig. S 4, provide specific surface areas of 35 ± 2 $m^2\,g^{-1}$ (pigments Yellow 1 and 2), 6 ± 1 $m^2\,g^{-1}$ (pigment Red 1), 10 ± 1 $m^2\,g^{-1}$ (pigment Red 2), 35 ± 2 $m^2\,g^{-1}$ (pigment Orange), and 0.5 ± 0.1 $m^2\,g^{-1}$ (pigments Black 1 and 2), indicating the lowest agglomeration for the yellow pigments and the highest for both black ones. These values are comparable to those found for the "intestine". It indicates a similar state of aggregation of the pigments in cell culture medium and the intestinal fraction.

3.3. Cellular uptake and transport

Another important question is the determination of the intestinal uptake and transport of E 172 pigments to evaluate their bioavailability. The Transwell® system is a well established *in vitro* model to simulate the uptake of substances into intestinal cells, namely differentiated Caco-2 cells and their transport through the intestinal barrier. The uptake and transport was quantified by the determination of the iron content of each compartment by element analysis, shown in Fig. 5. Regardless of the E 172 species, all samples quite consistently showed an uptake between 20 and 30% of the added Fe amount into the cellular fraction, representing the cellular fraction. The particles can be strongly attached onto the cells or internalized. The transport of almost all E 172 species did not remarkably exceed the Fe background. Only E 172 Orange showed a slightly higher barrier crossing, exceeding the other materials up to a transported fraction slightly in repeated independent experiments. The correct application of iron to each sample was confirmed by recovery experiments, shown in Fig. S 2.

3.4. Cellular effects

Cell viability was determined by MTT measurements. Fig. 6A shows the viability of proliferating Caco-2 cells after incubation with the 7 investigated E 172 food colorants, leading to no observable cytotoxicity up to concentrations of 100 µg Fe/mL. Only the positive control Triton X-100 led to strong cytotoxicity. Effects of E 172 on the viability of differentiated Caco-2 cells has been published before (Fig. A.13 in (Voss et al., 2020a)), demonstrating the absence of cytotoxicity up to 200 µg Fe/mL.

Cellular impedance is an indicator for cell health, proliferation and cell barrier integrity, which can be determined by the xCELLigence® method. In this study, the cellular impedance was determined for proliferating as well as for differentiated Caco-2 cells over a time period of 72 h after incubation (Fig. 6B-D). In Fig. 6B the normal behavior of control cells (gray line) can be seen, indicating cell proliferation depicted by a constant increase of cell indices for around 24 h, followed by a plateau phase after reaching confluency. Differentiated cells show a slight fluctuation around their plateau, indicated by almost constant cell index values. ZnO nanoparticles, used as positive control, depict the changes in cell indices under toxic conditions. After a short increase, the cell indices collapse and go down to almost zero. In Fig. 6C and D and Fig. S 3, the cellular impedance analyses of Caco-2 cells are shown after incubation with 3 different concentrations of the E 172 food pigments (5, 25 and 50 µg Fe/mL). With regard to the effects on proliferating Caco-2 cells, the E 172 pigments can be subdivided into two groups. Red 1 (Fig. 6C) together with Red 2 and Orange (Fig. S3) showed almost no influence on the growth and impedance of proliferating Caco-2 cells. The other pigments, Black 1 (Fig. 6D), Black 2, Yellow 1, and to a lesser extent Yellow 2 (Fig. S3) showed a normal growth and impedance of Caco-2 cells only at the lowest concentration of 5 µg Fe/mL. For higher concentrations, cells showed a growth delay and the cell indices reached the plateau much later. Nevertheless, there no toxicity was observable. None of the E 172 food pigments had notable influence on the cell impedance of differentiated Caco-2 cells.

4. Discussion

In the European Union, the application of iron-containing materials with the purpose of use as food colorants (E 172) was re-evaluated by EFSA in the year 2015 (EFSA Scientific Committee, 2015b). A major remaining ambiguity was that the material characteristics of food additives, including the particle size distribution and the nanoscaled fraction, have still not been comprehensively evaluated. The intentional addition of nanomaterials or the use of nanotechnologies during production has to be declared on the packaging of food products (European Commission, 2011), and such products have to be assessed as "novel foods" (European Commission, 2015). In the case of novel foods, nanoparticulate iron-containing products are already on the market with the aim of enhanced iron uptake (European Commission, 2022). Recently, a detailed guidance has been released for the intentional application of nanotechnologies the food and feed sector for production processes, packaging or for food quality purposes (EFSA Scientific Committee, 2021a). Nanoparticle applications in food are discussed in the scientific community (Bouwmeester et al., 2009; Vance et al., 2015). In addition to that, the EFSA has also lately formulated a guidance to materials, which contain a nano-scaled fraction, but not intentionally applied nanotechnologies or nanomaterials, which has been a regulatory gap before (EFSA Scientific Committee, 2021b). It has been shown that such nanoparticles can occur in food unintentionally and therefore reach the human gastrointestinal tract (Voss et al., 2020a; Yang et al., 2014). Likewise, the materials in this study contained relevant nanoparticulate fractions. After oral uptake, nanoparticles can show nano-specific physico-chemical properties (Oberdorster et al., 2005) and possibly enhance cellular uptake by so-called "trojan horse mechanisms" (Hsiao et al., 2015). However, up to now little is known about the influence of the digestion process on the fate of orally taken up iron oxide nanoparticles.

Therefore, we investigated the influence of digestion on food colorants, by using an *in vitro* digestion system mimicking all three intestinal fluids (saliva, gastric and intestinal juice). 0.33 mg Fe/mL were applied into 16 mL artificial saliva, which corresponds to the recommended maximum level of 6 mg per day for the daily intake of iron supplements (BfR, 2021). Artificial digestion is a widely used *in vitro* method which has been further specified and developed for the digestion of various nanoparticle species (Versantvoort et al., 2005; Bohmert et al., 2014; Sieg et al., 2017; Voss et al., 2019). For a profound investigation of nanoparticles, a setting of material characterization methods can be combined with the artificial digestion. In this study, we applied measurements of ion release to track dissolution and SAXS to observe

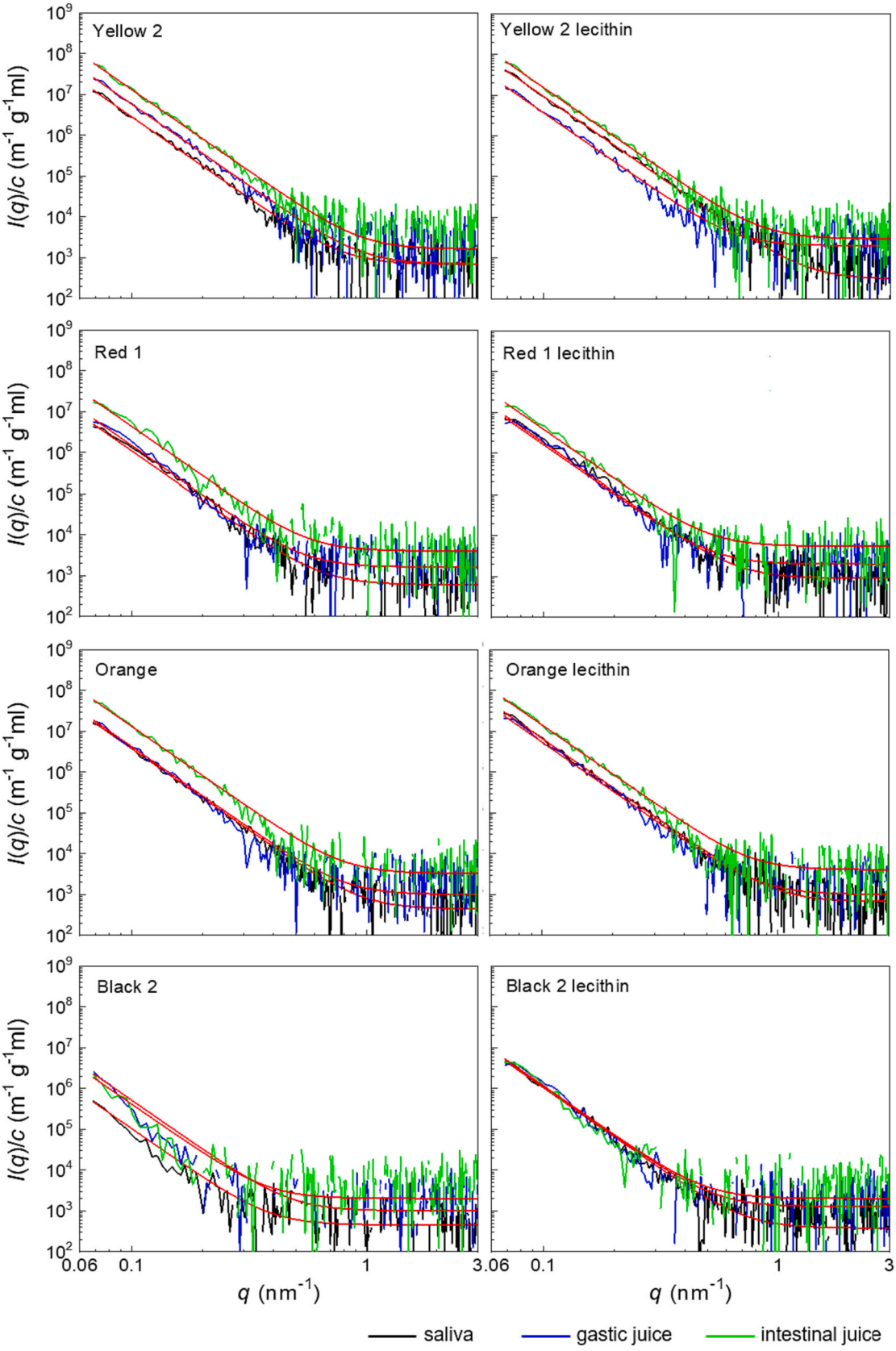

Fig. 3. SAXS data of pigments measured after incubation in saliva, stomach and intestine juice (black, blue and green lines, respectively) without (left) and with (right) lecithine. Curve fits employing Porod's law are provided (red solid lines). (For interpretation of the references to color in this figure legend, the reader is referred to the web version of this article.)

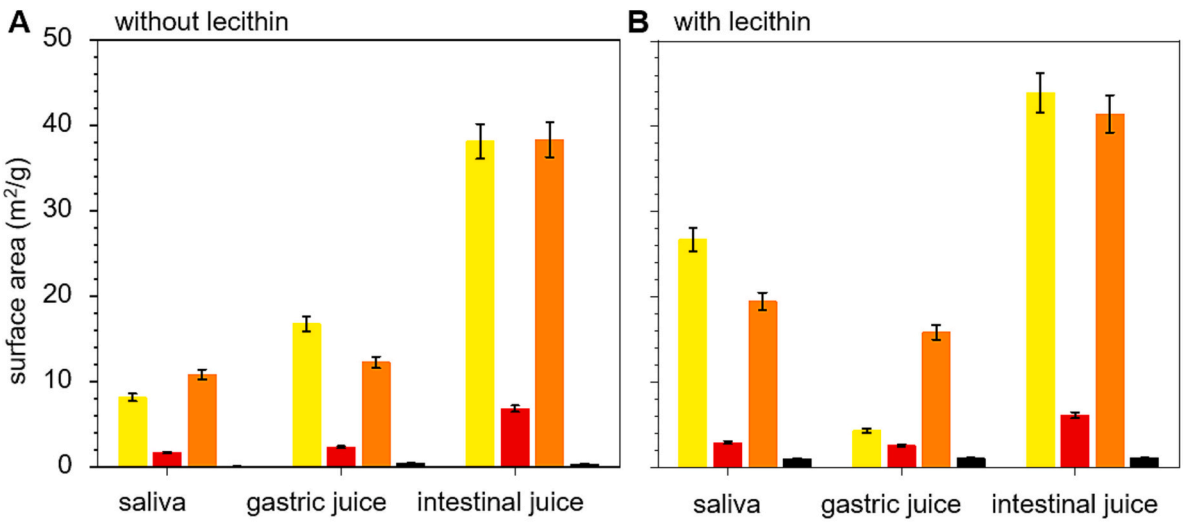

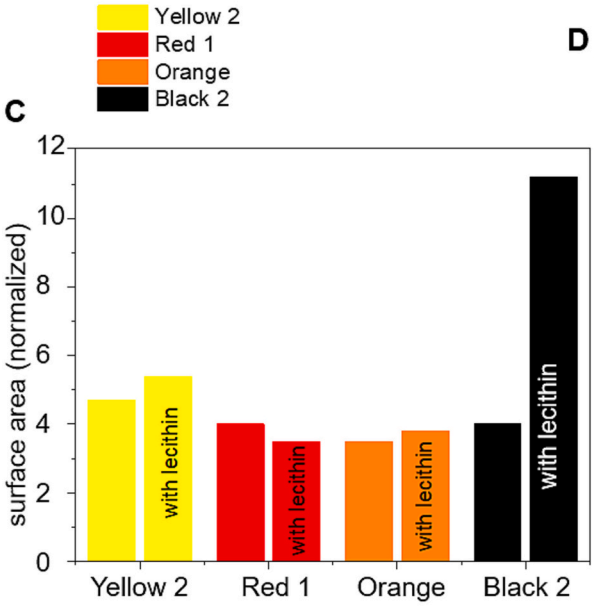

D

specific surface area of the pigments (m²/g)	without lecithin	with lecithin
Yellow 2		
saliva	8.2 ± 0.4	26.7 ± 1.4
gastric juice	16.8 ± 0.9	4.3 ± 0.2
intestinal juice	38.2 ± 2.0	44.0 ± 2.3
Red 1		
saliva	1.7 ± 0.1	2.9 ± 0.2
gastric juice	2.3 ± 0.2	2.6 ± 0.2
intestinal juice	6.9 ± 0.4	6.1 ±0.3
Orange		
saliva	10.9 ± 0.6	19.4 ± 1.0
gastric juice	2.3 ± 0.2	15.8 ± 0.9
intestinal juice	38.4 ± 2.1	41.5 ± 2.2
Black 2		
saliva	0.10 ± 0.01	0.10 ± 0.05
gastric juice	0.49 ± 0.03	1.07 ± 0.06
intestinal juice	0.39 ± 0.02	1.11 ± 0.06

Fig. 4. Specific surface areas of the pigments [A] without and [B] with added lecithin (upper and lower panel, respectively) after incubation in saliva, gastric and intestinal juice. [C] Specific surface areas of the pigments after intestinal digestion in relation to the specific surface area of the pigments in saliva without the presence of lecithin. For each pigment the left bar is the value without and the right bar is with added lecithin. [D] Table of specific surface areas of the pigments determined with SAXS after different steps of digestion. Values are given in $m^2\ g^{-1}$ of pigment.

particle stability and agglomeration behavior. Depending on the material, artificial digestion can strongly influence dissolution behavior of nanoparticles, measured by ion release. Some materials, like silver or aluminum nanoparticles show a low ion release (Lichtenstein et al., 2015; Sieg et al., 2017), where mostly a dissolution occurs in stomach fluid due to the acidic conditions, followed by reformation of particles in the intestinal fluid. Other materials, like zinc oxide dissolve almost completely in stomach fluid (Voss et al., 2019). Here, also single particles reemerge in the intestinal fluid. Also, *de novo* formation of nanoparticles from ions is possible (Juling et al., 2016; Kästner et al., 2018). For pristine particles in cell culture media, Sohal et al. found a very low ion release, consistent to our findings (Sohal et al., 2020). For digested iron oxide nanoparticles, previous studies showed a very ion release at each stage of the artificial digestion (Voss et al., 2021; Sohal et al., 2018a). Iron oxides were described to be very biodurable and persistent in saliva and stomach fluid. Only iron sulfate was predominantly dissolved in acidic stomach fluid. In contrast, "ultra small" iron oxide nanoparticles were found to be soluble to a high extent at pH 3 (Garcia-Fernandez et al., 2020). In the actual study, no material showed ion release of >1% in all digestive fluids with and without lecithin (Fig. 2). For comparison, also none of the materials showed ion release in water and cell culture medium, indicating a very low overall solubility. Previously, iron-containing engineered nanomaterials showed no ion release in water and different cell culture media (Voss et al., 2021). The

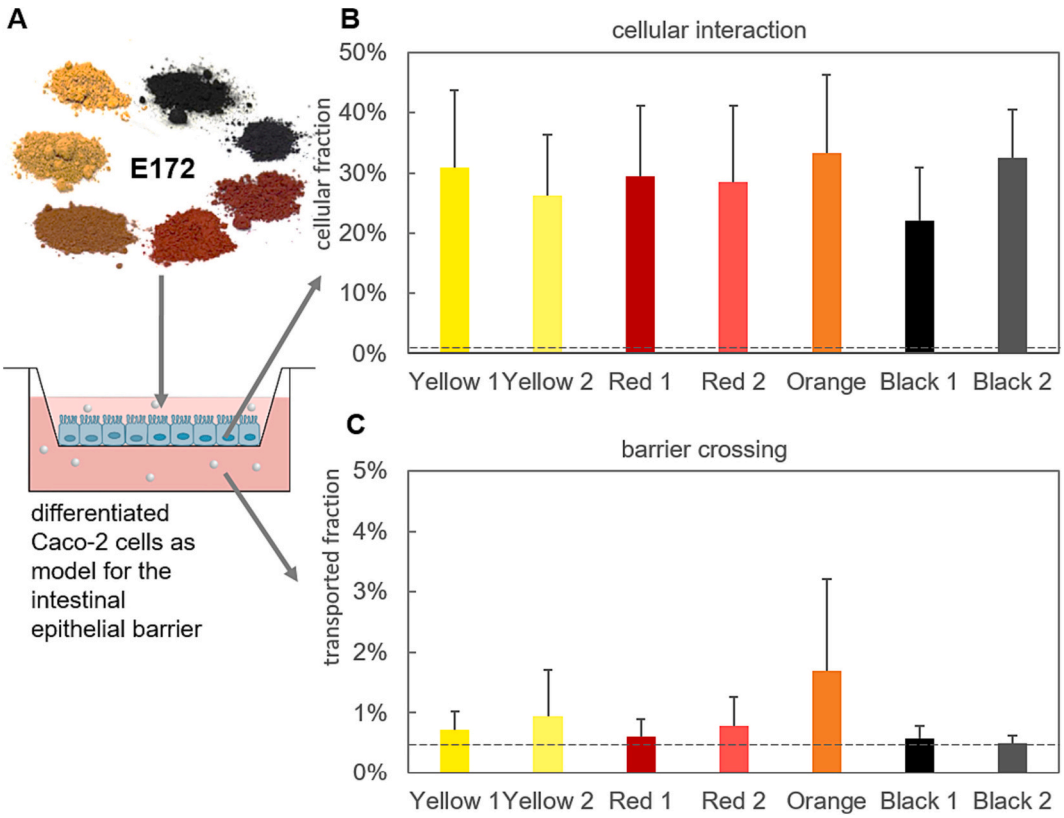

Fig. 5. Iron quantification from cellular uptake and transport studies, measured by AAS, measured as fraction compared to the theoretical added iron content from the E 172 samples. [A] depicts the scheme of a Transwell® system. Panel [B] indicates cellular interaction in the Transwell® membrane fraction and [C] shows iron in the basolateral fraction, indicating barrier crossing. The relative background iron content in cell culture medium is shown by dashed lines. Results are shown as mean values of at least 6 samples and error bars indicate standard deviation. Total iron recovery measurements are shown in Fig. S 2.

results with pigment Yellow 1, which was previously digested for method establishment, match nicely with the above observations, showing also no notable iron release during artificial digestion (Voss et al., 2021).

To complement the ion release measurements, SAXS results reveal information about particle stability and agglomeration status of the digested food colorants (Fig. 4). In all artificial fluids, the particles appear rather agglomerated, indicated by ratios of surface area to mass. Therefore, it was not possible to determine number-size-distributions of single particles. According to our findings, Yellow 2 and Orange tend to be less agglomerated, while Red1 and especially Black 2 have much smaller surface-area-to-mass ratios, speaking for higher agglomeration. The similar order of results was obtained for the pigments incubated in cell culture medium. Voss et al. showed by TEM and SAXS measurements, that Black 2 was also highly agglomerated as pristine particles (Voss et al., 2020a). Furthermore, the pigment Red 1 showed a low ratio of nanoparticles compared to larger particles, indicating relatively small amounts of single nanoparticles, probably also due to strong agglomerations. In this study, we have put a particular focus on the investigation of the influence of lecithin on the agglomeration behavior of the food colorants. Lecithin is authorized, according to the European Commission, as the food additive E322, which can be used as a food emulsifier, especially also as carrier additive to food colorants (European Commission, 2008). The emulsifying properties of lecithin are resulting from their amphiphilic properties, which can interact with organic as well as hydrophilic compounds and therefore influence the stability and agglomeration behavior of nanoparticulate substances in biological matrices (Deng, 2021). In saliva, the presence of lecithin resulted in deagglomeration. This underlines the properties of lecithin as an emulsifier. In intestinal juice, all particles showed the highest deagglomeration, indicating the presence of single nanoparticles in the small intestine after oral uptake and digestion. Sohal et al. showed a high agglomeration of iron oxide nanomaterials after artificial digestion, especially in the intestinal fluid (Sohal et al., 2018a). Previous studies with other digested nanoparticles showed both, particle formation and agglomeration as well (Sieg et al., 2017; Voss et al., 2019). At the intestinal stage, the effect of lecithin disappeared, probably due to digestion of lecithin by pancreatic lipases (Mellors and Tappel, 1967).

In addition to the investigation during digestion, we were interested in the behavior of the food colorants in *in vitro* intestinal models. Caco-2-based *in vitro* systems are frequently used as barrier models to simulate intestinal uptake and transport (Artursson and Karlsson, 1991) and are also able to take up nanoparticles (Hidalgo et al., 1989; Lichtenstein et al., 2017). Previous studies of Voss et al. showed a slight interaction of iron oxide nanoparticles with Caco-2 cells in a Transwell® system but no detectable barrier crossing (Voss et al., 2021). The cellular iron content was determined by element analysis, which does not allow to discriminate between cellular internalization and a robust cellular interaction, which is stable against washing procedures on the Transwell® membrane. In this study, the E 172 pigments show interactions of around 30% after an incubation time of 24 h with only minor differences among the chemical structures (Fig. 5). However, a transport through the epithelium was not measurable for the most materials. Only the orange pigment showed a slight transport, but still below 2% of the applied concentration and with a high error range. An available *in vivo* study with rats indicates a bioavailability between 0.2 and 9.4% of iron from orally administered iron oxide nanoparticles in liver, spleen and other organs, leading to elevated iron levels compared to bulk iron applications (Singh et al., 2013). Another study with chicken showed no particle uptake into liver and spleen, but an uptake of ionic iron in the cells of the intestine with an influence on iron uptake pathways, and the liver iron level, which indicates bioavailability of dissolved iron, probably

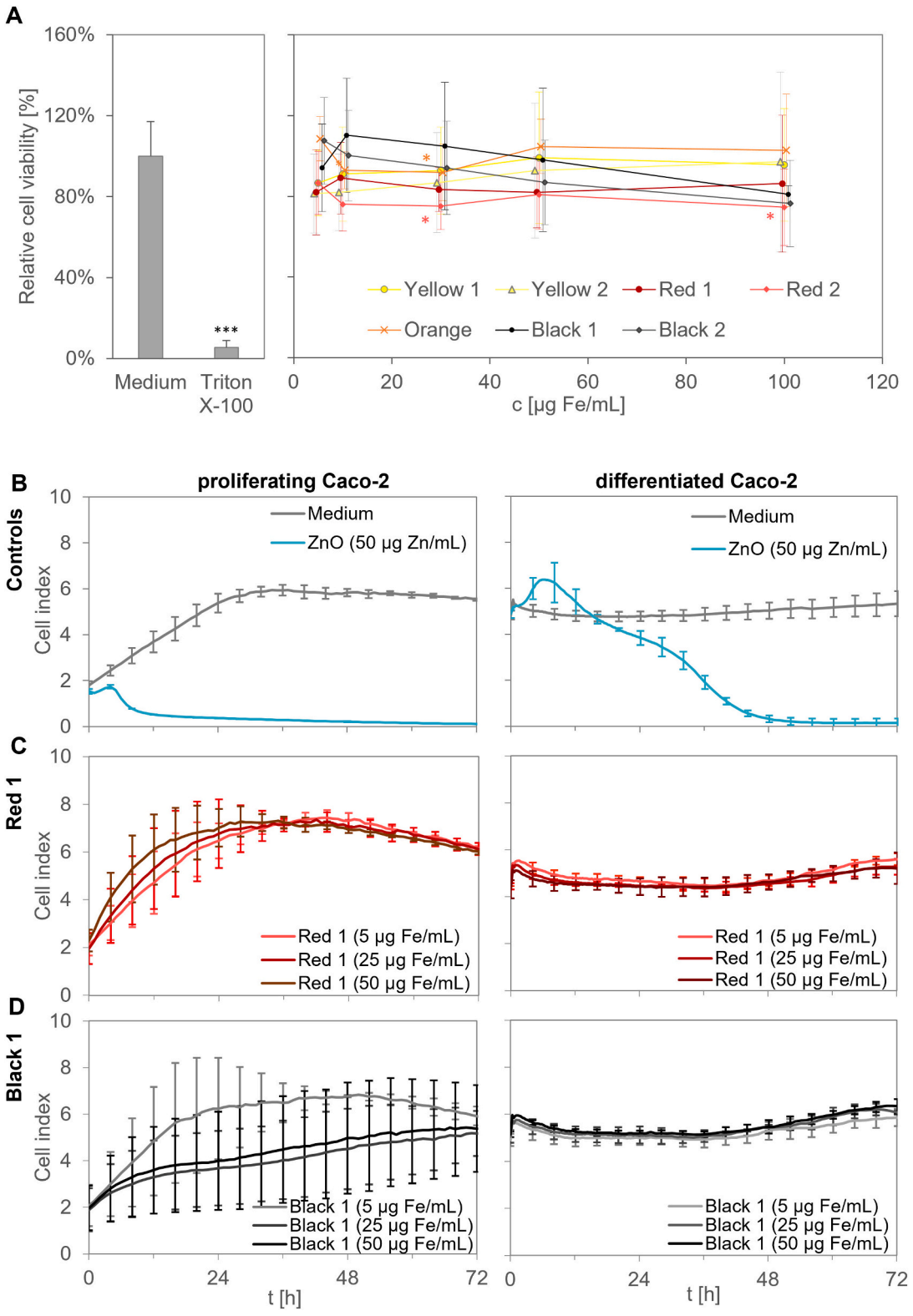

Fig. 6. [A] Viability of proliferating Caco-2 cells after 24 h incubation time with E 172 food colorants and controls, as determined by MTT assay. Food colorants were applied at iron concentrations of 5–100 µg Fe/mL. 0.01% Triton X-100 was used as toxic positive control. Results shown as mean values of at least 3 independent experiments with at least 3 replicates for each condition; error bars indicate standard deviation. Statistics were performed by Student's *t*-test compared to medium controls. Statistical significance is indicated by asterisks (* $p < 0.05$; ** $p < 0.01$; *** $p < 0.001$). [B—D] Cellular impedance of proliferating (left) and differentiated (right) Caco-2 cells, determined by xCELLigence® over a time period of 72 h after incubation with [B] controls and E 172 food colorants [C] Red 1 and [D] Black 1, with iron concentrations of 5, 25 and 50 µg Fe/mL. ZnO nanoparticles were used as a toxic positive control. The results are shown as mean cell indices of at least 3 replicates, and error bars indicate standard deviation. The results of the other E 172 food colorants are shown in Fig. S 3. (For interpretation of the references to color in this figure legend, the reader is referred to the web version of this article.)

due to the acidic digestive environment (Chamorro et al., 2015). While ionic iron can be taken up by iron transporters, iron particles can undergo endocytosis, but also non-endocytic uptake by direct access to the cytoplasm (Zanella et al., 2017). The lack of dissolution of particles here does not indicate an increased iron uptake *via* ionic transport mechanisms.

Iron is an important nutritional trace element with multiple essential functions in the human body, such as for oxygen binding in the hemoglobin protein, or to function as a cofactor in cytochrome. Given this importance for the human body, iron has a low toxic potential. However, some illnesses are known with relation to a lack of iron, such as iron deficiency anemia, but also with relation to an excess, like hemochromatosis (Anderson and Frazer, 2017). The latter happens often genetically caused or with relation to iron medication or excessive iron consumption resulting in symptoms like nausea, vomiting, gastrointestinal complaints or liver diseases (Musallam et al., 2013; Gaenzer et al., 2002; EFSA Scientific Committee, 2015a). There are only a few studies available, investigating the impact of nanoparticulate iron oxides on intestinal cells *in vitro* focusing on nano-specific effects of iron oxide particles are available (Sohal et al., 2018b). Structural changes in the Caco-2 cell monolayer and impact on tight junctions are described for haematite nanoparticles (Zhang et al., 2010; Kalive et al., 2012). Cellular metabolic disruption and elevated cytokine release was reported for iron oxide nanoparticles (Sohal et al., 2020). Garcia-Fernandez et al. showed no toxicity of iron oxide nanoparticles on Caco-2 and HT-29 cells after 48 h (Garcia-Fernandez et al., 2020). Although our results underline the general recognition, that the applied iron oxide particles do not carry a high risk for cell damage and acute toxicity, it is worth studying also possible cellular effects at subtoxic levels. Voss et al. investigated different engineered iron oxide nanoparticles, with all of them showing no acute toxicity on intestinal and hepatic cells, measured by various endpoints such as cell viability, oxidative stress or mitochondrial membrane potential (Voss et al., 2021). Some of the particles had an impact on caspase 3 and caspase 9 activation in HepaRG cells, related to apoptotic cell function. However, apoptosis induction was not observable by flow cytometry including Annexin-V staining. Furthermore cellular stress response was activated on RNA level, indicated by deregulation of the genes *BAD*, *DIABLO*, *FADD*, *TRADD* and *BCL2*. Some iron oxide particles showed a slight reduction of cellular ATP levels. At subtoxic levels, iron oxide nanoparticles had a strong influence on the gene expression of enzymes of xenobiotic metabolism in HepaRG cells, such as various cytochrome P450 (CYP) enzymes, but also phase II enzymes, solute carriers and ABC-transporters as well as the nuclear receptors AhR, PXR and CAR (Voss et al., 2020b). Oxidative stress response was indicated by deregulation of the genes *CAT*, but not on *HMOX1*. A yellow iron oxide nanomaterial induced a strong release of the cytokines IL-6 and IL-8, indicating inflammation. The particles had also influence on CYP protein quantity and CYP activity. It was not possible to draw mechanistic correlations between chemical structure and effects, but many effects were strongly pronounced for black Fe_3O_4 particles, while yellow and orange particles showed intermediate effects. Red particles caused the least effects on HepaRG cells. According to the recent results, we have no indications for further hazards caused by the food colorant compared to the previously tested particles. The here applied E 172 food colorants were already tested to be non-toxic on differentiated Caco-2 cells in a previous study (Voss et al., 2020a). Differentiated Caco-2 cells are often more robust with respect to the stable nature of their monolayer. In this study, also none of the food colorants showed an acute toxicity on proliferating Caco-2 cells, which are in general more susceptible for toxic effects (Fig. 6A). Cellular impedance measurements, which are more sensitive to minor changes in a real time cell analysis, reveal differences between the two cell types visible (Fig. 6B-D and Fig. S3). Again, the E 172 food colorants had no impact on differentiated Caco-2 cells. In contrast, on proliferating Caco-2 cells, the testing substances could be subdivided into two groups. While Red 1, Red 2 and Orange had no influence on cellular impedance, Yellow 1, Yellow 2, Black 1 and Black 2 caused a cellular growth delay at concentrations of 25 μg Fe/mL and higher. This growth delay could be mechanically driven by the presence of agglomerates. Sometimes, inert particles can impair cell viability just due to cellular overload, such as polystyrene particles did in experiments of Stock et al. (Stock et al., 2019). Stock et al. used several mg/mL for their experiments. The here applied concentrations, however, are not in overload conditions. An explanation is a real cellular impact on a subtoxic level. Likewise to the studies of Voss et al., here again the black and yellow food colorants were predominant in their effects, while the red ones showed the least (Voss et al., 2020b; Voss et al., 2021). Taken together, the nanoparticulate character of E 172 food colorants can have an impact on their gastrointestinal interaction and cellular effects.

5. Conclusion

Since it is known that commercially available and industrial as well as privately used E 172 iron oxide food colorants contain varying nanoparticulate fractions, the question became important, how these particles behave after oral ingestion in the gastrointestinal tract. The nanoparticulate character, the agglomeration behavior and the chemical material structure of E 172 food colorants could have an impact on gastrointestinal interaction and cellular effects. The dissolution of 7 differently structured iron-containing E 172 food colorants was negligible in water, cell culture medium and the three stages of the gastrointestinal tract (saliva, stomach fluid and intestinal fluid) according to an *in vitro* simulation. The specific surface areas of the pigments are relatively small, but differ considerably. This is the lowest for Black 2 and highest for Yellow 2. It is noteworthy that the specific surface areas of the digested materials generally increase from the saliva towards the intestine. The influence of lecithin on the increase in the specific surface area tends to be present, but less than might be expected due to its emulsifying properties. However, all materials showed strong interactions with cells of the intestinal barrier, simulated by differentiated Caco-2 cells. In contrast, a transepithelial transport of iron turned out to be very low. No particle species was toxic to Caco-2 cells up to an amount of 100 μg Fe/mL within 24 h. However, some materials (Yellow 1 + 2, Black 1 + 2) led to a growth delay of proliferating Caco-2 cells, while the others (Red 1 + 2, Orange) did not. None of the materials had an impact on the impedance of differentiated Caco-2 cells. Summed up, although there is a strong particle interaction with the cells of the intestinal barrier, almost no dissolution, transport and no acute cytotoxicity were observed.

Declaration of generative AI in scientific writing

No AI was used during the writing process.

Author contributions

Holger Sieg (HS), Caroline Schaar (CS), Nicole Fouquet (NF), Linda Böhmert (LB), Andreas F. Thünemann (AT), Albert Braeuning (AB).

Performed experiments (CS, NF, HS), Data evaluation (HS, CS, NF, AT), Writing the manuscript (HS, CS, NF, LB, AT), Project planning and discussion (HS, LB, AT, AB) Supervision and funding (AB). All authors have approved the final version of the manuscript.

Fundings

This publication is funded by the German Federal Institute for Risk Assessment Grant Numbers 1323–102 and 1322–782.

Declaration of competing interest

The authors declare no conflict of interest.

Data availability

Data will be made available on request.

Acknowledgements

We kindly acknowledge Marén Schlief and Sandra Graff for their help with the experimental work. We thank Maximilian Ebisch for SAXS experiments. We thank Anke Weißenborn and Linn Voss for scientific assistance and discussion.

Appendix A. Supplementary data

Supplementary data to this article can be found online at https://doi.org/10.1016/j.tiv.2024.105772.

References

Anderson, G.J., Frazer, D.M., 2017. Current understanding of iron homeostasis. Am. J. Clin. Nutr. 106, 1559S–1566S.
Artursson, P., Karlsson, J., 1991. Correlation between oral drug absorption in humans and apparent drug permeability coefficients in human intestinal epithelial (Caco-2) cells. Biochem. Biophys. Res. Commun. 175, 880–885.
BfR, 2021. Updated Recommended Maximum Levels for the Addition of Vitamins and Minerals to Food Supplements and Conventional Foods: BfR Opinion No 009/2021 of 15 March 2021. Bundesinst. für Risikobewertung, BfR-Stellungnahmen.
Bhattacharya, P.T., Misra, S.R., Hussain, M., 2016. Nutritional aspects of essential trace elements in oral health and disease: an extensive review. Scientifica 2016, 5464373.
Bohmert, L., Girod, M., Hansen, U., Maul, R., Knappe, P., Niemann, B., Weidner, S.M., Thunemann, A.F., Lampen, A., 2014. Analytically monitored digestion of silver nanoparticles and their toxicity on human intestinal cells. Nanotoxicology 8, 631–642.
Bouwmeester, H., Dekkers, S., Noordam, M.Y., Hagens, W.I., Bulder, A.S., De Heer, C., Ten Voorde, S.E., Wijnhoven, S.W., Marvin, H.J., Sips, A.J., 2009. Review of health safety aspects of nanotechnologies in food production. Regul. Toxicol. Pharmacol. 53, 52–62.
Bressler, I., Kohlbrecher, J., Thunemann, A.F., 2015. SASfit: a tool for small-angle scattering data analysis using a library of analytical expressions. J. Appl. Crystallogr. 48, 1587–1598.
Buhrke, T., Lengler, I., Lampen, A., 2011. Analysis of proteomic changes induced upon cellular differentiation of the human intestinal cell line Caco-2. Develop. Growth Differ. 53, 411–426.
Chamorro, S., Gutiérrez, L., Vaquero, M.P., Verdoy, D., Salas, G., Luengo, Y., Brenes, A., José Teran, F., 2015. Safety assessment of chronic oral exposure to iron oxide nanoparticles. Nanotechnology 26, 205101.
Cornell, R.M., Schwertmann, U., 2003. The Iron Oxides: Structure, Properties, Reactions, Occurrences, and Uses. Wiley-vch Weinheim.
Deng, L., 2021. Current progress in the utilization of soy-based emulsifiers in food applications-a review. Foods 10.
EFSA Scientific Committee, 2015a. Scientific opinion on dietary reference values for iron. EFSA Panel on Dietetic Products, Nutrition and Allergies (NDA) 13 (10), 4254.
EFSA Scientific Committee, 2015b. Scientific opinion on the re-evaluation of iron oxides and hydroxides (E 172) as food additives. EFSA J. 13, 4317.
EFSA Scientific Committee, 2021a. Guidance on risk assessment of nanomaterials to be applied in the food and feed chain: human and animal health. EFSA J. 19 (8), 6768.
EFSA Scientific Committee, 2021b. Guidance on technical requirements for regulated food and feed product applications to establish the presence of small particles including nanoparticles. EFSA J. 19, e06769.
Erdman, J.W., Macdonald, I.A., Zeisel, S.H., 2012. Present Knowledge in Nutrition. John Wiley & Sons.
European Commission, 2008. Regulation (EU) No 1333/2008 of the European Parliament and of the Council of 16 December 2008 on food additives. Off. J. Eur. Union 354, 16–33.
European Commission, 2011. Regulation (EU) No 1169/2011 of the European Parliament and of the Council of 25 October 2011 on the provision of food information to consumers. OJ L 304 22.11.2011, p. 18.
European Commission, 2015. Regulation (EU) 2015/2283 of the European Parliament and of the Council of 25 November 2015 on novel foods. OJ L 327, 11.12.2015, pp. 1–22.
European Commission, 2022. Commission Implementing Regulation (EU) 2022/1373 of 5 August 2022 authorising the placing on the market of iron hydroxide adipate tartrate as a novel food and amending Implementing Regulation (EU) 2017/2470. C/2022/5554, OJ L 206, 8.8.2022, pp. 28–33.
Fogh, J., Fogh, J.M., Orfeo, T., 1977. One hundred and twenty-seven cultured human tumor cell lines producing tumors in nude mice. J. Natl. Cancer Inst. 59, 221–226.
Gaenzer, H., Marschang, P., Sturm, W., Neumayr, G.Ü., Vogel, W., Patsch, J., Weiss, G.Ü., 2002. Association between increased iron stores and impaired endothelial function in patients with hereditary hemochromatosis. J. Am. Coll. Cardiol. 40, 2189–2194.
Garcia-Fernandez, J., Turiel, D., Bettmer, J., Jakubowski, N., Panne, U., Rivas García, L., Llopis, J., Sanchez Gonzalez, C., Montes-Bayón, M., 2020. In vitro and in situ experiments to evaluate the biodistribution and cellular toxicity of ultrasmall iron oxide nanoparticles potentially used as oral iron supplements. Nanotoxicology 14, 388–403.
Hidalgo, I.J., Raub, T.J., Borchardt, R.T., 1989. Characterization of the human colon carcinoma cell line (Caco-2) as a model system for intestinal epithelial permeability. Gastroenterology 96, 736–749.
Hsiao, I.L., Hsieh, Y.K., Wang, C.F., Chen, I.C., Huang, Y.J., 2015. Trojan-horse mechanism in the cellular uptake of silver nanoparticles verified by direct intra- and extracellular silver speciation analysis. Environ. Sci. Technol. 49, 3813–3821.
IOM, 2001. Dietary Reference Intakes for Vitamin A, Vitamin K, Arsenic, Boron, Chromium, Copper, Iodine, Iron, Manganese, Molybdenum, Nickel, Silicon, Vanadium, and Zinc. Institute of Medicine (US) Panel on Micronutrients. ISBN-10: 0–309–07279-4, ISBN-10: 0–309–07290-5.
ISO 17867, 2020. Particle size analysis — Small angle X-ray scattering (SAXS). Oct 5, 2020.
ISO 20804, 2022. Determination of the specific surface area of porous and particulate systems by small-angle X-ray scattering (SAXS).
ISO/FDIS 23484, 2022. Determination of particle concentration by small-angle X-ray scattering (SAXS).
JECFA, 1980. Twenty-Third Report of the Joint FAO/WHO Expert Committee on Food Additives.
Juling, S., Bachler, G., Von Gotz, N., Lichtenstein, D., Bohmert, L., Niedzwiecka, A., Selve, S., Braeuning, A., Lampen, A., 2016. In vivo distribution of nanosilver in the rat: the role of ions and de novo-formed secondary particles. Food Chem. Toxicol. 97, 327–335.
Kalive, M., Zhang, W., Chen, Y., Capco, D.G., 2012. Human intestinal epithelial cells exhibit a cellular response indicating a potential toxicity upon exposure to hematite nanoparticles. Cell Biol. Toxicol. 28, 343–368.
Kästner, C., Lampen, A., Thünemann, A.F., 2018. What happens to the silver ions? – silver thiocyanate nanoparticle formation in an artificial digestion. Nanoscale 10, 3650–3653.
Lands, R., Isang, E., 2017. Secondary hemochromatosis due to chronic oral iron supplementation. Case Rep. Hematol. 2017, 2494167.
Lichtenstein, D., Ebmeyer, J., Knappe, P., Juling, S., Bohmert, L., Selve, S., Niemann, B., Braeuning, A., Thunemann, A.F., Lampen, A., 2015. Impact of food components during in vitro digestion of silver nanoparticles on cellular uptake and cytotoxicity in intestinal cells. Biol. Chem. 396, 1255–1264.
Lichtenstein, D., Ebmeyer, J., Meyer, T., Behr, A.C., Kastner, C., Bohmert, L., Juling, S., Niemann, B., Fahrenson, C., Selve, S., Thunemann, A.F., Meijer, J., Estrela-Lopis, I., Braeuning, A., Lampen, A., 2017. It takes more than a coating to get nanoparticles through the intestinal barrier in vitro. Eur. J. Pharm. Biopharm. 118, 21–29.
Mcdowell, L.A., Kudaravalli, P., Sticco, K.L., 2018. Iron Overload.
Mellors, A., Tappel, A.L., 1967. Hydrolysis of phospholipids by a lysosomal enzyme. J. Lipid Res. 8, 479–485.
Musallam, K.M., Cappellini, M.D., Taher, A.T., 2013. Iron overload in β-thalassemia intermedia: an emerging concern. Curr, Opin. Hematol., p. 20
NanoGenoTOX, 2011. NanoGenoTOX Report. http://www.nanogenotox.eu/files/PDF/Deliverables/nanogenotox%20deliverable%203_wp4_%20dispersion%20protocol.pdf;Stand13.03.2017.
Oberdorster, G., Oberdorster, E., Oberdorster, J., 2005. Nanotoxicology: an emerging discipline evolving from studies of ultrafine particles. Environ. Health Perspect. 113, 823–839.
Oberdorster, G., Oberdorster, E., Oberdorster, J., 2007. Concepts of nanoparticle dose metric and response metric. Environ. Health Perspect. 115, A290.
Orthaber, D., Bergmann, A., Glatter, O., 2000. SAXS experiments on absolute scale with Kratky systems using water as a secondary standard. J. Appl. Crystallogr. 33, 218–225.
Porod, G., 1951. Die Rontgenkleinwinkelstreuung Von Dichtgepackten Kolloiden Systemen. 1. Kolloid-Zeitschrift and Zeitschrift Fur Polymere, 124, pp. 83–114.
Ray, P.C., Yu, H., Fu, P.P., 2009. Toxicity and environmental risks of nanomaterials: challenges and future needs. J. Environ. Sci. Health C Environ. Carcinog. Ecotoxicol. Rev. 27, 1–35.
Sieg, H., Kastner, C., Krause, B., Meyer, T., Burel, A., Bohmert, L., Lichtenstein, D., Jungnickel, H., Tentschert, J., Laux, P., Braeuning, A., Estrela-Lopis, I., Gauffre, F., Fessard, V., Meijer, J., Luch, A., Thunemann, A.F., Lampen, A., 2017. Impact of an artificial digestion procedure on aluminum-containing nanomaterials. Langmuir 33, 10726–10735.
Sieg, H., Braeuning, C., Kunz, B.M., Daher, H., Kastner, C., Krause, B.C., Meyer, T., Jalili, P., Hogeveen, K., Bohmert, L., Lichtenstein, D., Burel, A., Chevance, S., Jungnickel, H., Tentschert, J., Laux, P., Braeuning, A., Gauffre, F., Fessard, V., Meijer, J., Estrela-Lopis, I., Thunemann, A.F., Luch, A., Lampen, A., 2018. Uptake and molecular impact of aluminum-containing nanomaterials on human intestinal caco-2 cells. Nanotoxicology 12, 992–1013.
Singh, S.P., Rahman, M.F., Murty, U.S.N., Mahboob, M., Grover, P., 2013. Comparative study of genotoxicity and tissue distribution of nano and micron sized iron oxide in rats after acute oral treatment. Toxicol. Appl. Pharmacol. 266, 56–66.
Sohal, I., Kwan Cho, Y., O'fallon, K., Gaines, P., Demokritou, P., Bello, D., 2018a. Dissolution behavior and biodurability of ingested engineered nanomaterials in the gastrointestinal environment. ACS Nano 12, 8115–8128.
Sohal, I.S., O'fallon, K.S., Gaines, P., Demokritou, P., Bello, D., 2018b. Ingested engineered nanomaterials: state of science in nanotoxicity testing and future research needs. Part. Fibre Toxicol. 15, 1–31.
Sohal, I.S., Deloid, G.M., O'fallon, K.S., Gaines, P., Demokritou, P., Bello, D., 2020. Effects of ingested food-grade titanium dioxide, silicon dioxide, iron (III) oxide and zinc oxide nanoparticles on an in vitro model of intestinal epithelium: comparison between monoculture vs. a mucus-secreting coculture model. NanoImpact 17, 100209.

Stock, V., Bohmert, L., Lisicki, E., Block, R., Cara-Carmona, J., Pack, L.K., Selb, R., Lichtenstein, D., Voss, L., Henderson, C.J., Zabinsky, E., Sieg, H., Braeuning, A., Lampen, A., 2019. Uptake and effects of orally ingested polystyrene microplastic particles in vitro and in vivo. Arch. Toxicol. 93, 1817–1833.

Vance, M.E., Kuiken, T., Vejerano, E.P., Mcginnis, S.P., Hochella Jr., M.F., Rejeski, D., Hull, M.S., 2015. Nanotechnology in the real world: redeveloping the nanomaterial consumer products inventory. Beilstein J. Nanotechnol. 6, 1769–1780.

Versantvoort, C.H., Oomen, A.G., Van De Kamp, E., Rompelberg, C.J., Sips, A.J., 2005. Applicability of an in vitro digestion model in assessing the bioaccessibility of mycotoxins from food. Food Chem. Toxicol. 43, 31–40.

Voss, L., Saloga, P.E.J., Stock, V., Böhmert, L., Braeuning, A., Thünemann, A.F., Lampen, A., Sieg, H., 2019. Environmental impact of ZnO nanoparticles evaluated by in vitro simulated digestion. ACS Appl. Nano Mater. 3, 724–733.

Voss, L., Hsiao, I.L., Ebisch, M., Vidmar, J., Dreiack, N., Böhmert, L., Stock, V., Braeuning, A., Loeschner, K., Laux, P., Thünemann, A.F., Lampen, A., Sieg, H., 2020a. The presence of iron oxide nanoparticles in the food pigment E172. Food Chem. 127000.

Voss, L., Yilmaz, K., Burkard, L., Vidmar, J., Stock, V., Hoffmann, U., Pötz, O., Hammer, H.S., Peiser, M., Braeuning, A., Löschner, K., Böhmert, L., Sieg, H., 2020b. Impact of iron oxide nanoparticles on xenobiotic metabolism in HepaRG cells. Arch. Toxicol. 94 (12), 4023–4035.

Voss, L., Hoché, E., Stock, V., Böhmert, L., Braeuning, A., Thünemann, A.F., Sieg, H., 2021. Intestinal and hepatic effects of iron oxide nanoparticles. Arch, Toxicol.

Yameen, B., Choi, W.I., Vilos, C., Swami, A., Shi, J., Farokhzad, O.C., 2014. Insight into nanoparticle cellular uptake and intracellular targeting. J. Control. Release 190, 485–499.

Yang, Y., Doudrick, K., Bi, X., Hristovski, K., Herckes, P., Westerhoff, P., Kaegi, R., 2014. Characterization of food-grade titanium dioxide: the presence of nanosized particles. Environ. Sci. Technol. 48, 6391–6400.

Zanella, D., Bossi, E., Gornati, R., Bastos, C., Faria, N., Bernardini, G., 2017. Iron oxide nanoparticles can cross plasma membranes. Sci. Rep. 7, 11413.

Zhang, W., Kalive, M., Capco, D.G., Chen, Y., 2010. Adsorption of hematite nanoparticles onto Caco-2 cells and the cellular impairments: effect of particle size. Nanotechnology 21, 355103.

Zimmermann, M.B., Hilty, F.M., 2011. Nanocompounds of iron and zinc: their potential in nutrition. Nanoscale 3 (6), 2390–2398.